دوازدهمین کنگره ملی سراسری
فناوریهای نوین در حوزه توسعه پایدار ایران
12th National Congress of
the New Technologies in Sustainable Development of Iran
senaconf.ir

Smart Polymeric Nanocomposite Based on Protonated Aluminosilicate, Curcumin, and Chitosan for Mesalamine Drug Delivery as an Anti-inflammatory Nanocarrier

Forough Amiry, Mohammad Reza Sazegar*, Ali Mahmoudi

Faculty of Chemistry, North Tehran Branch, Islamic Azad University, Hakimiyeh, Tehran, Iran.

*Corresponding author e-mail: m_r_sazegar@yahoo.com

Abstract

Due to the importance of the colon-specific disease, its treatment with reduced side effects has become fascinating over the last decades. The aim of this study was the synthesis of the nanocomposite based on the protonated aluminum-modified mesoporous silica nanoparticles (H/Al-MSN) and curcumin possesses mesalamine to develop its efficacy and eliminating side effects for enhancing permeability in intestinal tissues. Here, different amounts of mesalamine were loaded and studied under accurate analysis in order to evaluate release quality. The aluminosilicate nanoparticles are encapsulated by the combination of curcumin as an herbal product and also chitosan as a natural biopolymer with the advantages of non-toxicity, biocompatibility, biodegradability, and non-allergenic. The release of mesalamine from the nanocomposite was investigated in different pH included acidic, neutral, and alkaline media. The results showed that the release of mesalamine is dependent on acidity. A colonic drug delivery system was designed based on the release time and pH sensitivity. The drug release was studied at pH 5.5, 7, and 8 a different region of the gastrointestinal tract was simulated. The results showed

that the trend of mesalamine release is higher at pH 8 with high efficacy performance of more than 90 percent at room temperature for about 90 h.

Keywords: Mesalamine; Aluminosilicate; Drug delivery; colon-specific disease; Anti-inflammatory; Mesoporous silica nanoparticles.

Introduction

The overall prevalence rate for inflammatory bowel disease (IBD) in the world is 6.8 million and high rates has been reported in the industrial areas [1]. The reason why IBD occurs is still a mystery but researchers believe that some factors such as geographical location, inappropriate diet, genetics, and inappropriate immune conditions can be attributed to this prevalence [2]. Despite several ways that have been reported to treat IBD, they have not been quite successful. That's an essential reason that needs to find therapy for this disease is becoming more important every day. IBD treatments may involve using a suitable diet, drug therapy, or in some cases surgery. Using anti-inflammatory drugs are often the first step to treat Crohn's disease (CD) and Ulcerative-Colitis (UC) [3]. Mesalamine with the other name of mesalazine and the chemical name of 5-aminosalicylic acid with three function groups of amine, carboxylic acid, and phenolic groups (Scheme 1) is used for the treatment of inflammatory bowel disease, such as Crohn's disease and ulcerative colitis. This drug generally applied for moderately disease. Mesalamine (5-ASA) is a cyclo-oxygenase inhibitor and anti-inflammatory drug to manage both UC and CD disorders, all the same, it is the first drug in the treatment of UC [4]. As this drug is a kind of rapidly absorbed medicine by the small intestine so it needs to develop a colon-specific delivery system that is able to enhance its therapeutically efficacy and reduce the side effects [5].

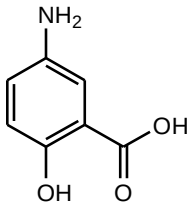

Scheme 1. Mesalamine chemical structure

Planet extracted medicines like curcumin have also anti-inflammatory effects [6]. Curcumin is a polyphenol extracted from the rhizome of Curcuma longa (turmeric). This material has been used traditionally as a medicine for the treatment of a large range of illnesses, such as infectious diseases, inflammation, and blood disorders, hepatic, and gastric. Low cost, minimal side effects, and abundance of Curcumin are the benefit.[7] Existence of biological properties such as sustainability, chemical flexibility, human and eco-friendliness in natural polymers like curcumin and chitosan is the reason of popularity of them in drug delivery system [8].

Chitosan as a versatile natural biopolymer is a great selection for curcumin encapsulation by dint of its biodegradability, biocompatibility, non-toxicity, and non-allergenic. The cationic character like of Chitosan is related to the primary amino group which is responsible for several advantages of this polymer such as controlled drug delivery, mucoadhesion, in situ gelation, transfection, enhancement of, and efflux pump inhibitory properties [9]. Plant based medicines are used as biomedical treatments from ancient time. Nowadays we use them instead or over synthetic drugs because herbal drugs have lesser side effects comparing with chemical synthesized medicines. Novel Drug Delivery System (NDDS) play essential roles in increasing the efficacy of plant drugs and solving some problems such as slow efficacy of herbal drugs, poor stability in gastric environment, high extent of first metabolism, and etc. [10].

An ideal colon targeting system is a type of system which deliver a therapeutic agent, selectively and effectively, to the colon. Colon-specific drug delivery systems perfectly sustain the drug release in the upper GI tract (stomach and small intestine), while triggering the drug release in the colon [11].

Nanotechnology and Nanomaterial drug delivery systems are rapidly developing where materials in the nanoscale range are applied to deliver the therapeutic agents to targeted sites in a controlled manner or as means of diagnostic tools. Chemotherapeutic agents, biological agents, immunotherapeutic agents are the recent outstanding applications of nanomedicine in the treatment of various diseases [12].

Oral colon-specific drug delivery system (OCDD) has become more advance as a site-specific drug delivery system using nanomaterials over the past decade. The use of this system helps us to control drug release in the gastrointestinal (GI) track by the combination of one or more controlled mechanisms. This mechanism leads to the release of drugs in the upper part of GI track, but rapidly release in the colon. Due to approximately low proteolytic enzyme activities existence and completely long transit time, the Colon has been mentioned to be the optimal absorption site for protein and polypeptides after oral administration [13,14].

Enteric-coated systems (ECS) are frequently used for colonic drug delivery. PH difference between small intestine and colon is not really marked, so this can be a kind of disadvantage for PH dependent approaches. The time-dependent systems also have some limitations; the inability to any variation in the upper gastrointestinal track transit time, and also any variation in gastric discharge time may be caused to start on drug release in the small intestine before reaching the colon [15].

Mesoporous silica nanoparticles are the mesoporous form of silica that recently have developed in the nanomaterial field. Mesoporous silica nanoparticles (MSNs) as carriers for colonic drug delivery has been introduced for their application as a promising platform in the medical field in recent decades. MSN has been widely used to develop drug delivery strategy in the field of nanotechnology [16]. The large surface area, high pore size and pore volume, hydrothermal resistance, non-toxicity, safe carriers, considerable biocompatibility and biodegradability, uniform aqueous dispersion are the inherent properties of MSNs that introduce these nanoparticles the great candidate as carriers for the colonic drug delivery. The pure and modified MSN for possessing the

range of pore size between 2 and 50 nm are the suitable platforms for the biomedical application and drug delivery systems [17-18]. They can be easily synthesized using sol-gel technique so producing it cost effective. Besides, the morphology, pore size and volume and particle size can be appropriately transformed by parameters control during synthesis [19].

Some studies show that the GO nanoparticle platform which contains a grafted cell-targeting functionality also can be used for the activation of pharmaceutical ingredients used in magnetothermal therapy [20]. In addition, graphene oxide, when conjugated with ciprofloxacin, exhibits low cytotoxicity and high stability and shows antimicrobial activity [21].

The aim of this study was to synthesis a nanocomposite based on mesoporous silica nanoparticles modified with the active ingredient curcumin and natural chitosan polymer which its structure was evaluated by FTIR, XRD, nitrogen adsorption-desorption, SEM, and TEM analysis. The release ability of mesalamine was investigated in different PH which is explained in detail.

Experimental

Materials and methods

Tetraethyl orthosilicate (TEOS), (3-Aminopropyl) Trithoxysilane (APTES), Aluminum chloride, Cetrimonium Bromide (CTAB), Hydrochloride Acid (HCL), Sodium Hydroxide (NaOH), Sodium Hydroxide (NaOH), and Ammonia, were purchased from Merck Company. Mesalamine was prepared from Hakim Pharmaceutical Company in Tehran, Iran. Curcumin and chitosan were purchased from Sina Daru Company.

Synthesis of mesoporous silica nanoparticles (MSN)

A suitable amount of CTAB (12 g) was poured into distilled water (200 ml) in an Erlenmeyer (250 ml) flask and magnetically stirred. After 30 min, the Ammonia Ethanol solution which contained Ammonia 25% (20 ml) in of Ethanol (30 ml) was added continuously to the container of CTAB till the solution became clear. Then added TEOS (25 ml) to the stirring solution and stirred for 4

h. At the end left in static for 24 h. The sediments were then filtered and washed with 200 ml Ethanol and distilled water. Afterward, the sediments were dried at 110 °C and weighed. The materials were then calcined at 550°C for 3 h. This was denoted as MSN [22].

Synthesis of H/Al-MSN

The amount of MSN (2.7 g) was stirred with distilled water (50 ml) in a beaker for 15 min. After that an aqueous solution of the aluminum nitrate with the initial molar ratio of Si/Al=20 was added to the mixture and stirred continues for 24 h at room temperature. The results were centrifuged and washed with distilled water (20 ml) followed by dried at 90 °C and then calcined at 550 °C for 3 h. after that, the obtained powder was added to a 3% sulfuric acid solution and stirred for 3 h and then filtered, washed with distilled water (30 ml) and dried in an oven at 90 ^{o}C for 5 h. The product was denoted as H/Al-MSN. The XRF analysis showed the Si/Al molar ratio of 18.9 for H/Al-MSN.

A protocol for the synthesis of H/Al-MSN-Mes (Loading of mesalamine)

Dispersed the specified weighted H/Al-MSN (1 g) in ethanol (30 ml) and sonicated for 20 min. Different concentrations of the ethanolic mesalamine solutions (included 0.1, 0.15, and 0.2 % mesalamine, respectively, in a 20 ml ethanol) were added separately and then stirred in a 60°C water bath for 14 h. The products were washed twice with ethanol (20 ml) and distilled water (20 ml), separately, followed by centrifuged and then dried in an oven at 60 ^{o}C for 10 h. The light pinkish powder was denoted as H/Al-MSN-Mes.

A common protocol for the synthesis of AMCC

The amount of chitosan (0.5 g) dissolved with distilled water (30 ml) and then defined amount of curcumin (0.05 g) was added and magnetically stirred at room temperature for 2 h. The mixture was represented as Chs-Cur. After that, the synthesized Chs-Cur was added to the H/Al-MSN-Mes

with different mesalamine concentrations of 0.1, 0.15, and 0.2 % and were magnetically stirred for 3 h. The materials were then centrifuged and washed with ethanol (20 ml) and dried up. This final product is denoted as AMCC.

Mesalamine release under different acidity

The release of mesalamine was evaluated in three different pH (acidic, alkaline, and neutral). The aqueous solutions were 50 ml and the amount of investigated AMCC were 0.05 g for each samples. The assay was performed at room temperature.

The absorbance of the mesalamine remaining in the supernatant was measured using UV-vis spectroscopy at 230 nm. The amount of mesalamine adsorbed onto nanocomposites of AMCC and adsorption efficiency were calculated using Equations (1) and (2), respectively:

$$M_e = \frac{(C_0 - C_e)}{m} \times V \quad (1)$$

$$AEC\% = \left(\frac{C_0 - C_e}{C_e}\right) \times 100 \quad (2)$$

Where M_e *(mg/g)* is an amount of mesalamine adsorbed at the equilibrium state, *AEC%* is an Adsorption Efficiency Coefficient, C_0 (mg/L) is an initial mesalamine concentration, C_e (mg/L) is a mesalamine concentration at equilibrium state, *V (L)* is a volume of mesalamine solution, and *m (g)* is the mass of the nanocomposite used.

Nanocomposites characterization

Fourier transform infrared (FTIR) measurements of the nanocomposites were carried out using an Agilent Carry 640 FTIR spectrometer. Nitrogen physisorption analysis was conducted on a Quantachrome Autosorb-1 at 77 K. Before the measurement, the samples were evacuated at 573

K for 3 h. The crystallinity of nanocomposites was measured with a Bruker Advance D8 X-ray powder diffractometer with Cu K_α (l = 1.5418 Å) radiation as the diffracted monochromatic beam at 40 kV and 40 mA. The morphology of the nanocomposites were studied from scanning electron microscope (SEM). A scanning electron microscope equipped with an energy dispersion X-ray spectrometer (EDX) was conducted on SEM (JEOL JSM-6701 F) to observe the morphology as well as to obtain the elemental analysis of the nanocomposites using. Before observation by SEM-EDX, the sample was coated by Pt using a sputtering instrument. The measurement of mesalamine was occurred using UV-Vis spectrophotometer model UV-1800, Shimadzu, Kyoto, Japan. The bulk Si/Al molar ratio of 20 was determined by Bruker S4 Explorer X-ray fluorescence spectroscopy (XRF) using Rh as anode target material operated at 20 mA and 50 kV. XRF analysis reported the Si/Al molar ratio of 18.9.

Result and Discussion

Characterization of the nanocomposites

The pure MSN was prepared by using the sol-gel method and the AMCC nanocomposites were synthesized through the post-synthesis technique using aluminum nitrate, mesalamine, curcumin, and chitosan, respectively. The Si/Al molar ratio of 18.9 was obtained and the different concentrations of 0.1, 0.15, and 0.2% mesalamine were used to prepare of the AMCC nanocomposites.

Fig. 1 shows the FTIR spectroscopy of the pure MSN and the three nanocomposites of AMCC (0.1 %), AMCC (0.15 %), and AMCC (0.2 %) at the range is 400-4000 cm^{-1}. The functional groups among variant AMCC with the different mesalamine concentrations can be identified using FT-IR spectroscopy. The non-acidic silanol groups (Si-OH) or water molecules (OH) that remained on the pure MSN surface were observed as a broad band at the range of 3100–3600 cm^{-1}.

The AMCC samples represented the wide bonds at the range of 2700-3600 cm^{-1} attributed to the presence of the carboxylic group in their structures. A various number of hydrogen bonding due to the presence of the carboxylic, phenolic, and the amine groups resulted in the formation of the broad bands at this area for the nanocomposite samples. The sharp peaks at 3430 cm^{-1} showed the presence of amine group in the AMCC nanocomposites. Two bands at the regions of 2910 and 2860 cm^{-1} are attributed to the C-H stretching bands due to the existence of curcumin and chitosan in the nanocomposite structures [23, 24].

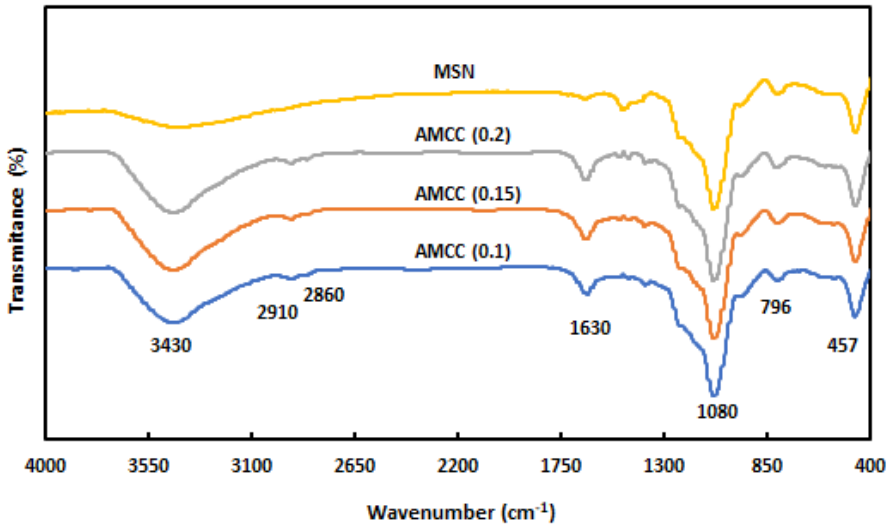

Fig. 1 FTIR spectra of MSN, and AMCC (0.1, 0.15, 0.2 g) at the region of 400-4000 cm^{-1}

The strong peak at 1080 cm^{-1} and the medium peak at 457 cm^{-1} attributed to the stretching vibration of the Si-O-Si bond, while two peaks of 796 and 1630 cm^{-1} are related to the bending vibration of the Si-O-Si bond. Moreover, the peak of 1630 cm^{-1} shows the N-H bending vibration corresponding to the mesalamine as well as chitosan structures in the AMCC nanocomposites. Incorporating aluminum in the MSN structure resulted in vibration at around 457 cm^{-1} that has been covered by the stretching vibration of the Si-O-Si bond [24].

Fig. 2 shows the low-angle XRD pattern for the pure MSN and the AMCC nanocomposites with different concentrations of mesalamine (0.1, 0.15, and 0.2 %) at the range of 0^{o} -10^{o}. XRD patterns

of MSN clearly showed the ordered mesoporous silica structure through the presenting of four diffraction peaks indexed as 100, 110, 200, and 210 at the low angle degree of 1.5-5.1° in terms of 2θ. They are illustrated the presence of a 2D hexagonal framework with a d_{100}-spacing of around 3.4 nm. The loading aluminum atoms accompanied with the mesalamine molecules into the pure MSN, and after that encapsulation with two bulky components of curcumin and chitosan has shifted the intense peak of 100 from 1.5° for MSN to the higher degree of 1.85° for all the nanocomposite samples. Simultaneously, all of these four diffraction peaks drastically were decreased so especially the peaks of 110, 200, and 210 approximately were disappeared which this phenomenon indicated the essential disordering into the nanocomposite structures.

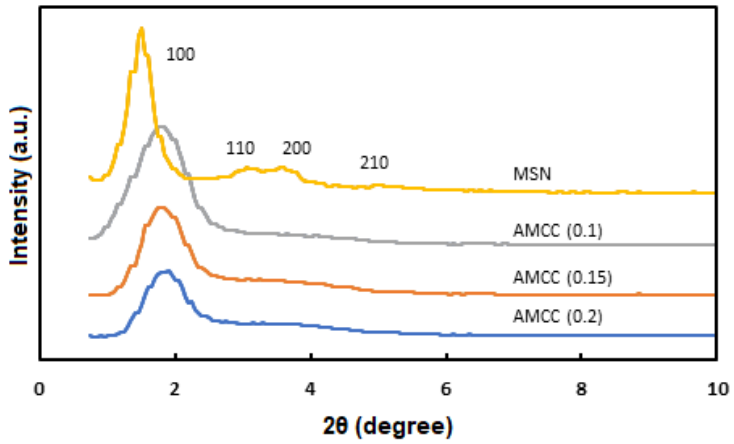

Fig. 2 XRD patterns of the pure MSN and the AMCC (0.1, 0.15, and 0.2) nanocomposites at the low-angle degree of 0°-10°.

On the other hand, the change appearances in the peak heights and locations of the XRD pattern confirmed the formation of the three nanocomposites with irregular silica mesoporous structures. The results of XRD patterns exhibited that the intensity of the highest peak (100) more decreased with increasing the mesalamine concentration. Therefore, the crystallinity of the nanocomposites more led to the less ordered structure with increasing mesalamine species [25].

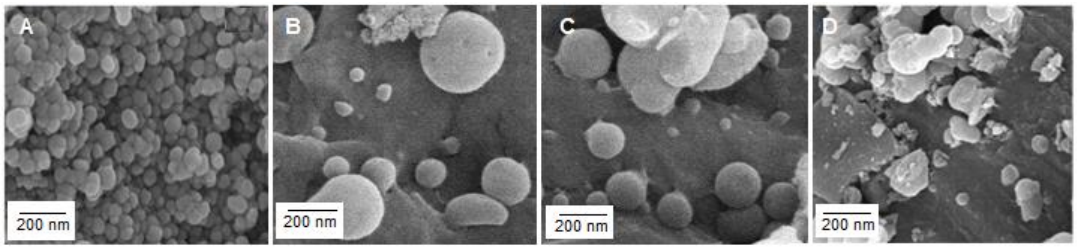

Fig. 3 SEM images of the (A) MSN, (B) AMCC (0.1), (C) AMCC (0.15), and (D) AMCC (0.2) samples

The morphology of the pure MSN and the AMCC (0.1), AMCC (0.15), and AMCC (0.2) nanocomposites have exhibited by SEM images [14] that is shown in Fig. 3. The image of 3A is belong to the MSN which presented a fairly uniform spherical particles with average particle sizes of 70-150 nm. The synthesized AMCC nanocomposites showed the fragment-like morphology with larger and less uniform spherical particles and large chitosan-curcumin fragments are well seen in the SEM images.

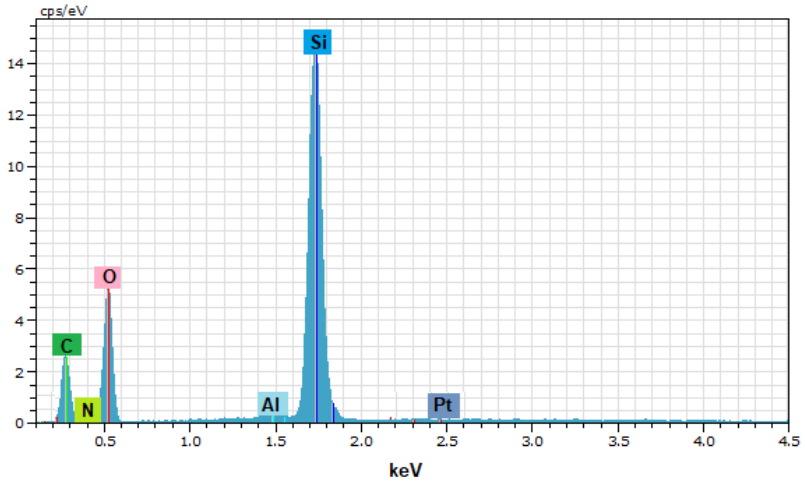

Fig. 4 Energy-dispersive X-ray spectroscopy of the AMCC (0.1) sample

As a symbolic sample, the EDX analysis of the AMCC (0.1) nanomaterial is shown in Fig. 4, indicated to the presence of silicon, aluminum, carbon, nitrogen and oxygen.

Table 1 physical characteristics of the MSN and AMCC samples

Sample	***S*** **(m^2/g)**	***Vp*** **(cm^3/g)**	***W*** **(nm)**
MSN	998	0.82	3.34
AMCC (0.1)	581	0.35	2.89
AMCC (0.15)	493	0.25	2.30
AMCC (0.2)	365	0.22	1.64

S., BET surface area (m^2/g) obtained from N_2 adsorption; V_p, total pore volume (ml/g); *W*, pore size (nm) obtained from BJH method.

Table 1 presents the distinguishable difference in the surface area, pore size, and volume of the MSN, AMCC (0.1), AMCC (0.15), and AMCC (0.2). A decrease in the surface area was observed from 998 m^2g^{-1} for MSN to 493 m^2g^{-1} for the AMCC (0.2) is due to the occupation of the MSN surface area by the various species such as aluminum, mesalamine, curcumin, and chitosan. The blockage of the pores with the mentioned materials resulted in a decrease in the pore volumes from 0.82 cm^3g^{-1} for MSN to 0.3 cm^3g^{-1} for the AMCC (0.2). As similar to the pore volume, the pore size also has been decreased from 3.34 to 1.26 nm for the MSN and AMCC (0.2), respectively. Therefore, the results showed that the reduced trend of the surface area, pore volume and size directly is related to the increase in the mesalamine amount.

The loading curcumin and chitosan components, accompany by mesalamine and aluminum could affect the reduction of these physical properties [26].

Fig. 5A and 4B show nitrogen adsorption-desorption isotherms and pore size distributions of the MSN and AMCC (0.1, 0.15, QND 0.2) samples, respectively. The nitrogen sorption isotherm of these nanomaterials showed type IV isotherms with H4 hysteresis loops which indicated to the presence of the porous nanomaterials [27]. The isotherm of the MSN and AMCC nanocomposites exhibited the characteristic of the sharp infection of the capillary condensation with almost uniform pore structures at a relative pressure of around 0.1-0.3 that indicated the presence of the uniform mesoporous structures [28].

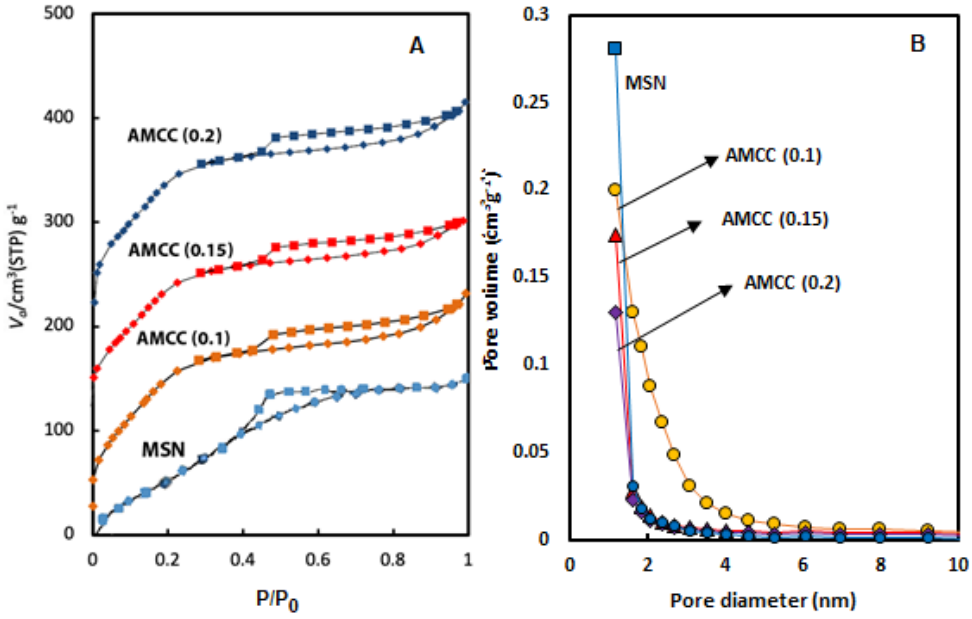

Fig. 5 (A) Nitrogen sorption isotherms and (B) pore size distribution for the MSN, AMCC (0.1), AMCC (0.15), and AMCC (0.2) samples.

The isotherms at higher relative pressure of 0.9-1.0 exhibited a slow increase in the adsorbed nitrogen that is an evidence to the existence of the week extra-framework structure. The moderate nitrogen adsorption in the relative pressure at the range of 0.3-0.9 showed the uniform microporous

structures in the nanocomposites which described a 2D porous structure for these nanomaterials. Fig. 5B described the narrow pore size distributions at the pore diameters around 1-3 nm. The proposed schematic chemical structure of the AMCC nanocomposite was exhibited in Scheme 1. In this structure, the protonated Al-MSN has bonded to mesalamine through hydrogen bonding and this fragment also is bonded to the curcumin and chitosan molecules.

Loading efficiency of mesalamine into the H/Al-MSN sample

In mesalamine delivery process, the mesalamine loading capacity of the H/Al-MSN nanostructures was investigated. The storage of mesalamine in the modified nanostructures was studied through the UV monitoring of the mesalamine solution.

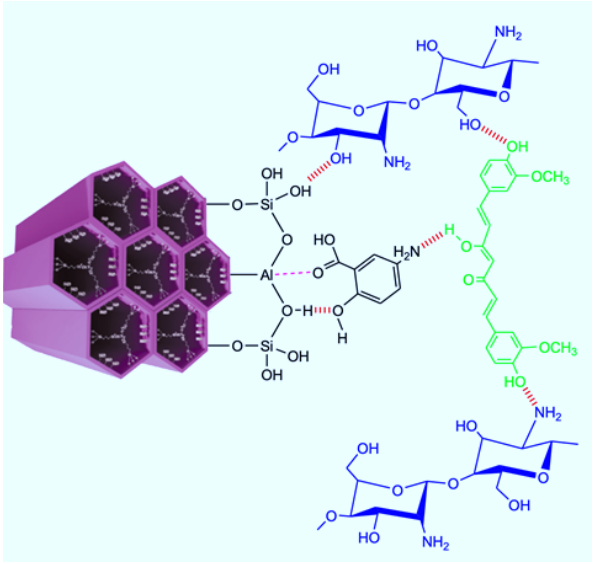

Scheme 1. Suggested chemical structure for the AMCC nanocomposite

The color of the pure mesalamine solution in ethanol was pinkish and after the reaction between different concentration of mesalamine and H/Al-MSN, the color of the solution became light pinkish while the white powder of H/Al-MSN changed to the light pinkish color. The loading

efficiency of the mesalamine adsorbed on the H/Al-MSN surface is one of the important factors for the bio-application of nanomaterials that was calculated using equation 1 [29]. The results showed that the loading efficiency of mesalamine on the H/Al-MSN surface was a mesalamine concentration-dependent process. There was an optimum concentration of mesalamine absorbed on the H/Al-MSN surface. The initial concentration of mesalamine was 7 mg/mL, which the highest loading efficiency were 73, 80, and 85% for the samples of 0.01, 0.02, and 0.03 g, respectively (Fig. 6).

This means that the drug loading efficiency of mesalamine has been dependent on the drug concentrations, nanoparticles concentrations, and the media acidity [30]. The adsorption process of mesalamine onto the H/Al-MSN is related to the electrostatic interactions between the drug and catalyst. Therefore, the anti-inflammatory drug of mesalamine can be efficiently absorbed onto the H/Al-MSN surface. To establish a therapeutic platform, the synthesized nanocomposites should be checked with the biomedical experiments.

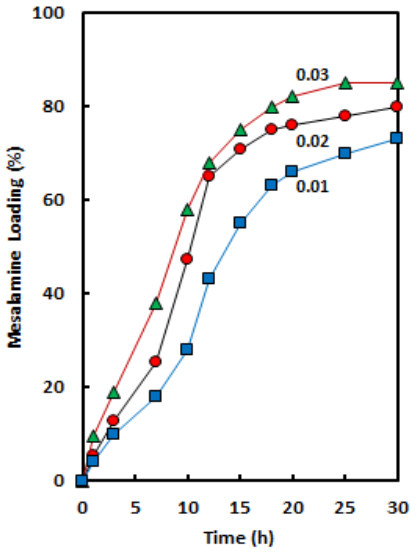

Fig. 6 The loading process of the different concentrations of mesalamine on the H/Al-MSN surface

Release efficiency of mesalamine from the AMCC nanocomposites

The in vitro anti-inflammatory drug-release of mesalamine of the AMCC nanocomposites was demonstrated under three different media pH in Fig. 7. The release of mesalamine from the AMCC nanocomposites included the different loaded anti-inflammatory drug (0.1, 0.15, and 0.2%) was investigated in the pH of 5.5, 7, and 8. The released mesalamine from the AMCC nanocomposites was monitored using UV-vis spectroscopy in the different acidic media at pH 5.5, 7, and 8.

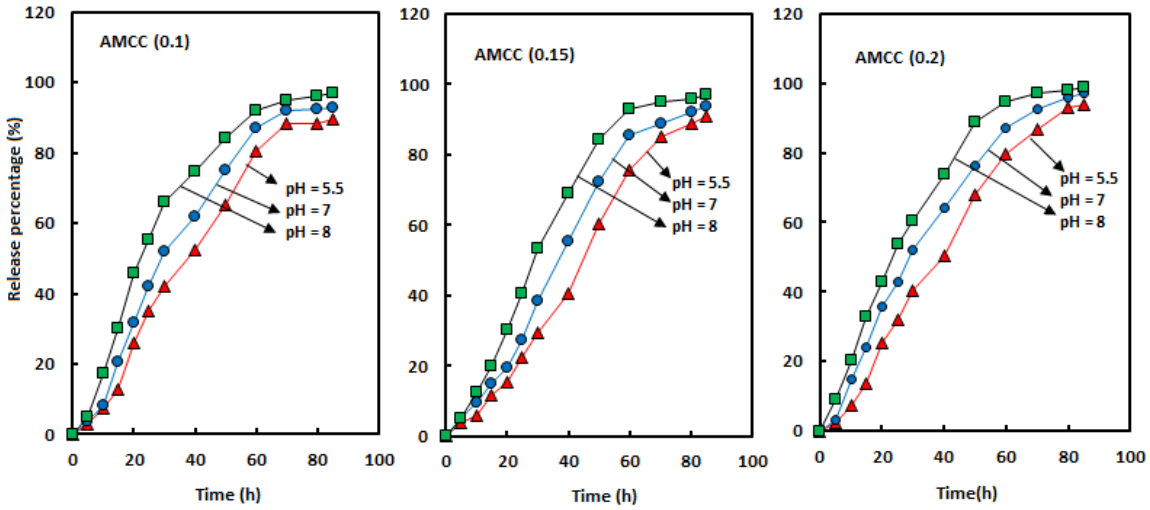

Fig. 7 Mesalamine release profile of the AMCC (0.1, 0.15, and 0.2) in different pH media of 5.5, 7, and 8 at room temperature.

Table 2 shows the maximum release of mesalamine from the AMCC(0.1), AMCC(0.15), and AMCC(0.2) nanocomposites. The results showed that release rate of this anti-inflammatory drug from the AMCC samples at pH 8 is higher than that at pH 5.5 and 7 at around 80 h. This means that the amount of mesalamine concentrations have an important rolls in the release rate of mesalamine. It can be seen the AMCC samples included 0.2% mesalamine exhibited higher drug release in comparison with the AMCC samples containing the 0.1 and 0.15% mesalamine.

The trend of the drug release at pH 8 can be divided into two sections including the initial 60 h and the section between 60-80 h. While the release percentage of 92.3, 93.1, and 94.6% were observed for the AMCC(0.1), AMCC(0.15), and AMCC(0.2) samples, respectively, after 60 h, these percentages entered the stable stage of slow release and revealed 97.4, 98.6, and 99.3%, respectively, after 80 h for the mentioned AMCC samples.

Table 2 The maximum of mesalamine release from the AMCC nanocomposites at pH 5.5, 7, and 8 at room temperature after 80 h

Sample	pH 5.5	pH 7	pH 8
AMCC (0.1)	89.5	93.2	97.4
AMCC (0.15)	91.2	94.3	98.6
AMCC (0.2)	94.7	97.1	99.3

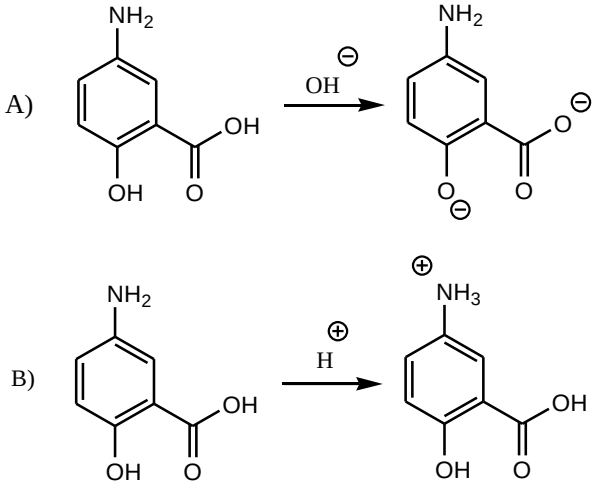

Scheme 2 the ionic structures of mesalamine molecule in the alkaline (A) and acidic (B) medium

The drug release observed at pH 5.5 and 7 were the slow processes in these two release steps. The chemical structure of mesalamine in an alkaline medium forms an ionic compound with two ionic centers, consequently it can better dissolve through the hydration process in the aqueous medium (scheme 2). This phenomenon may be to the attraction of the ionic mesalamine and aqueous solution at high pH values [31]. Therefore, the AMCC nanostructures are pH-responsive systems for mesalamine delivery and suitable way for the inflammatory therapy. In an acidic liquid medium, mesalamine molecules are protonated and form stronger bonds with aluminum as Lewis acid, resulting in slower and less release of mesalamine.

Conclusion

In this study, the AMCC nanocomposites were successfully prepared based on protonated aluminosilicate nanoparticle with the high drug loading efficiency in order to decrease the side effects of mesalamine as an anti-inflammatory drug. Here, we used curcumin as a natural anti-inflammatory drug and also used the natural polymer of chitosan for the treatment of colonic disease. The characterization of the intermediate nanoparticles and nanocomposites were carried out using several methods such as FTIR spectroscopy, XRD patterns, SEM images, and nitrogen adsorption-desorption isotherms. The activity of the synthesized nanomaterials were investigated in vitro conditions in the different environments included acidic, neutral, and alkaline media. This evaluation can be led to the finding a pathway for mesalamine release in gastrointestinal tissues. The drug release was investigated with accuracy in different PH. The results showed that the trend of mesalamine release is higher at the pH 8 with high efficacy performance more than 90 percentage at room temperature for about 90 h.

Acknowledgments

We thanks to Islamic Azad University, Dept. of Chemistry for all support from this study.

Disclosure

The authors report no conflicts of interest in this work.

References

[1] Kaur G, Singh K, et al. Development of modified apple polysaccharide capped silver nanoparticles loaded with mesalamine for effective treatment of ulcerative colitis. *J drug deliv sci tech*. 2020; 60: 1-10.

[2] Seydian SS, Nokhostin F, et al. A review of the diagnosis, prevention, and treatment methods of inflammatory bowel disease, *J Med Life*. 2019; 12:113-122.

[3] Kefalakes H, Stylianides TJ, et al. Exacerbation of inflammatory bowel disease associated with the use of nansteroidal anti-inflammatory drugs. *Eur J Clin pharmacol*. 2009; 65: 963-970.

[4] Wei Wang, Ren X, et al. Hierarchical mesoporous silica microspheres prepared by partitioned cooperative self-assembly process using sodium silicate as precursor and their drug release performance. *Microporous Mesoporous Mater*. 2019; 275: 50-60.

[5] Jafari S, Derakhshankhah H, et al. Mesoporous silica nanoparticles for therapeutic, diagnostic application. *Biomed Pharmacother*. 2019; 109: 1100-1111.

[6] Kocaadam B, Sanlier N. Curcumin, An active component of Tomeric (Curcuma longa), and its effects on health. *Crit Rev Food Sci Nutr*. 2017; 2; 57: 2889-2895.

[7] Ghosh S, Banerjee S, et al. The beneficial role of curcumin on inflammation, diabetes and neurodegenerative disease. *Food Chem Toxicol*. 2015; 83: 111-124.

[8] Ngwuluka NC, Ochekpe NA, et al. Naturapolyceutics, The Science of Utilizing Natural Polymers for Drug Delivery. *Polymers*. 2014; 6: 1312-1332.

[9] Schnurch AB, Dunnhaupt S. Chitosan-based drug delivery systems. *Eur J Pharm Biopharm*. 2012; 81: 463-469.

[10] Hu Q, Luo Y. Chitosan-based nanocarriers for encapsulation and delivery of curcumin. *Int Biol Macromol*. 2021; 179: 125-135.

[11] Bayan M F, Bayan RF. Recent advance in mesalamine colonic delivery systems. *Future J Pharm Sci*. 2020; 6: 43.

[12] Verma H, Prasad SB, et al. Herbal drug delivery systems. *Int J Curr Pharm Rev Res*. 2013; 4: 88-101.

[13] Liu L, Fishman ML, et al. Pectin-based system for colon specified drug delivery via oral route. *Biomaterials*. 2003; 24: 3333-3343.

[14] Yang L, Chu JS, et al. Colon-specific drug delivery, new approaches and in vitro, in vivo evaluation. *Int J Pharm*. 2002; 235: 1-15.

[15] Patel NV, Patel JK, et al. Design, development and in vitro evaluation of Mesalamine tablets containing Pectin and Chitosan for colon-specific drug delivery. *Pharmascope*. 2010; 1: 94-102.

[16] Kinget R, Kalala W, et al. Colonic drug targeting. J Drug Target. 1998; 6: 129-149.

[17] Aghayan M, Mahmoudi A, et al. A novel colorimetric sensor for naked-eye detection of cysteine and Hg2+ based on "on–off" strategy using Co/Zn-grafted mesoporous silica nanoparticles. *Dalton Trans Advance Article*. 2021.

[18] Aghayan M, Mahmoudi A, et al. Fe(III) porphyrin metal organic framework as an artificial enzyme mimics and its application in biosensing of glucose and H_2O_2. *J Porous Mater*. 2019; 26: 1507-1521.

[19] Hajiagha NG, Mahmoudi A, et al. Synthesis of cobalt-modified MSN as a model enzyme, Evaluation of the peroxidatic performance. *Microporous and Mesoporous Mater*. 2019; 274: 43-53.

[20] Pramanik N, Ranganthan S, et al. A composite of hyaluronic acid-modified graphene oxide and iron oxide nanoparticles for targeted drug delivery and magnetothermal therapy, ACS Omega, 4 (2019) 9284-9293.

[21] Kooti M, Sedeh AN, et al. Magnetic graphne oxide inlaid with silver nanoparticles as antibacterial and drug delivery composite, Appl. Microbiol. Biotechnol, 102 (2018) 3607-3621.

[22] Narayan R, Nayak UY, et al. Mesoporous silica Nanoparticles, *Pharmaceutics*. 2018; 10: 118.

[23] Tayefe HC, Sazegar MR, et al. Co/Zn-Grafted Mesoporous Silica Nanoparticles Catalyzed Cyclohexanimine Oxidation under UV Irradiation, High Performance Ozonation Process. *Electron Mater Lett*. 2021; 13: 677–686.

[24] Sazegar MR, Dadvand A, et al. Novel protonated Fe-containing mesoporous silica nanoparticle catalyst, excellent performance cyclohexane oxidation. *RSC Adv*. 2017; 7: 27506–27514.

[25] Sazegar MR, Jalil AA, et al. Protonation of Al-grafted mesostructured silica nanoparticles (MSN), Acidity and catalytic activity for cumene conversion. *Chem Eng J*. 2014; 240: 352–361.

[26] Kamarudin NHN, Jalil AA,et al. Elucidation of acid strength effect on ibuprofen adsorption and release by aluminated mesoporousilica nanoparticles. *RSC Adv*. 2015; 5: 30023-30031.

[27] Jamshidi D, Sazegar MR. Antibacterial Activity of a Novel Biocomposite Chitosan/Graphite Based on Zinc-Grafted Mesoporous Silica Nanoparticles. *Int J Nanomedicine*. 2020; 15: 871-883.

[28] Noghreiyan AV, Sazegar MR, et al. Investigation the emission spectra and cytotoxicity of TiO_2 and Ti-MSN/PpIX nanoparticles to induce photodynamic effects using X-ray. *Photodiagnosis Photody Ther*. 2020; 30: 101770.

[29] Zhao J, Yang H, et al. Fabrication of pH-responsive PLGA(UCNPs/DOX) nanocapsules with upconversion luminescence for drug delivery. *Sci Rep*. 2017; 7: 18014.

[30] Wang X, Li F, et al. Ambient aqueous synthesis of ultrasmall Ni0.85Se nanoparticles for noninvasive photoacoustic imaging and combined photothermalchemotherapy of cancer. *ACS Appl Mater*. 2017; 9: 41782-41793.

[31] Jia X, Yin J, et al. Polyacrylic acid modified upconversion nanoparticles for simultaneous pH-triggered drug delivery and release imaging. *J Biomed Nanotechnol*. 2013; 9: 2063-2072.